

Renormalization-group computation of the critical exponents of hierarchical spin glasses: Large-scale behavior and divergence of the correlation length

Michele Castellana^{1,2} and Giorgio Parisi¹¹*Dipartimento di Fisica, Università di Roma "La Sapienza," I-00185 Rome, Italy*²*Laboratoire de Physique Théorique et Modèles Statistiques (LPTMS), CNRS and Université Paris-Sud, UMR8626, Bâtiment 100, F-91405 Orsay, France*

(Received 5 November 2010; published 29 April 2011)

In a recent work [M. Castellana and G. Parisi, *Phys. Rev. E* **82**, 040105(R) (2010)], the large-scale behavior of the simplest non-mean-field spin-glass system has been analyzed, and the critical exponent related to the divergence of the correlation length has been computed at two loops within the ϵ -expansion technique by two independent methods. By performing the explicit calculation of the critical exponents at two loops, one obtains that the two methods yield the same result. This shows that the underlying renormalization group ideas apply consistently in this disordered model, in such a way that an ϵ -expansion can be set up. The question of the extension to high orders of this ϵ -expansion is particularly interesting from the physical point of view. Indeed, once high orders of the series in ϵ for the critical exponents are known, one could check the convergence properties of the series, and find out if the ordinary series resummation techniques, yielding very accurate predictions for the Ising model, work also for this model. If this is the case, a consistent and predictive non-mean-field theory for such a disordered system could be established. In that regard, in this work we expose the underlying techniques of such a two-loop computation. We show with an explicit example that such a computation could be quite easily automatized, i.e., performed by a computer program, in order to compute high orders of the ϵ -expansion, and so eventually make this theory physically predictive. Moreover, all the underlying renormalization group ideas implemented in such a computation are widely discussed and exposed.

DOI: [10.1103/PhysRevE.83.041134](https://doi.org/10.1103/PhysRevE.83.041134)

PACS number(s): 05.20.-y, 75.10.Nr, 64.60.ae

I. INTRODUCTION

Spin glasses, structural glasses, and the physical description of their critical properties have interested statistical physicists for several decades. The mean-field theory of these models [1–4] provides a physically and mathematically rich picture of their physics and of their critical behavior. Notwithstanding the great success of such mean-field theories, real spin-glass systems are non-mean-field systems, because they have short-range interactions. It follows that these systems cannot be described by mean-field models. As a matter of fact, the generalization of the above mean-field theories to the non-mean-field case is an extremely difficult task that has still not been achieved, so that the development of a predictive and consistent theory of glassy phenomena for real systems is still one of the most hotly debated and challenging problems in this domain [5–11].

There are several reasons why this task is so difficult to achieve. For example, the standard field-theoretical techniques [12,13], yielding the Ising model critical exponents with striking agreement with experimental data, usually do not apply to locally interacting glassy systems. Indeed, a considerable difficulty in the setup of a loop expansion for a spin glass with local interactions is that the mean-field saddle point has a very complicated structure [3], and could even be nonuniquely defined. It follows that the predictions of a loop expansion performed around one selected saddle point could actually depend on the choice of the saddle point itself [14], resulting into an intrinsic ambiguity in the physical predictions of such an expansion. Moreover, nonperturbative effects are poorly understood and not under control, and the basic properties of the large-scale behavior of these systems

are still far from being clarified. From the physical point of view, the fact that one cannot handle perturbatively corrections to the mean-field solution could imply that the physics of real systems is radically different from the mean-field one, so that a completely new description is needed.

The physical properties of the paramagnetic-ferromagnetic transition emerge in a clear way in ferromagnetic systems, as was already discussed in the original work of Wilson [13], where one can write a simple renormalization group (RG) transformation, describing a flow under length-scale reparametrizations. These RG equations turn out to be exact in models with power-law ferromagnetic interactions built on hierarchical lattices such as the Dyson model [15,16]. As a matter of fact, in these models one can explicitly write an exact RG transformation for the probability distribution of the magnetization of the system. All the relevant physical information on the paramagnetic, ferromagnetic, and critical fixed point, and the existence of a finite-temperature phase transition are encoded into these RG equations. Moreover, all the physical RG ideas emerge naturally from these recursion relations, whose solution can be explicitly built up with the ϵ -expansion technique [16–18]. The convergence properties of such an ϵ -expansion in the Dyson model have been investigated in Ref. [17]. It turns out that the ϵ series is divergent, but can be made convergent with a suitable resummation technique.

The extension of this approach to random systems has been performed only for some particular models. On the one hand, a RG analysis for random models on the Dyson hierarchical lattice has been done in the past [19,20], and a systematic analysis of the physical and unphysical infrared (IR) fixed points has been performed within the ϵ -expansion technique.

Unfortunately, in such models spins belonging to the same hierarchical block interact with each other with the same [19] random coupling J , in such a way that frustration turns out to be relatively weak, and they are not a good representative of a realistic strongly frustrated system.

On the other hand, models with local interactions on hierarchical lattices built on diamond plaquettes [21] have been widely studied in their spin-glass version, and also lead to weakly frustrated systems even in their mean-field limit [22]. Notwithstanding this, such models yield a very useful and interesting playground to show how to implement the RG ideas in disordered hierarchical lattices, and in particular on the construction of a suitable decimation rule for a frustrated system, which is one of the basic topics in the construction of a RG for spin glasses, and so in the identification of the existence of a spin-glass phase in finite dimension.

In addition, recently there has been a new wave of interest for strongly frustrated random models on hierarchical lattices [23–25]: For example, it has been shown [24] that a generalization of the Dyson model to its disordered version [the hierarchical random energy model (HREM)] has a random energy model-like phase transition, yielding interesting new critical properties that do not appear in the mean-field case.

In a recent work [26], we performed a field theory analysis of the critical behavior of a generalization of Dyson’s model to the disordered case, known as the hierarchical Edwards-Anderson model (HEA) [23], that is physically more realistic than the HREM and presents a strongly frustrated non-mean-field interaction structure, being thus a good candidate to mimic the critical properties of a real spin glass. This analysis is based on the replica method, and in particular on the assumption that the physics of the system is encoded in the $n \rightarrow 0$ -limit [1,2]. Moreover, the symmetry properties of the HEA make a RG analysis simple enough to be performed with two independent methods, to check if the IR limit of the model is physically well defined independently on the computation technique that one uses. Another element of novelty of the HEA is that its hierarchical structure makes the RG equations simple enough to make a high-order ϵ -expansion eventually tractable by means of a symbolic manipulation program, resulting in a quantitative theory for the critical exponents beyond mean field for a strongly frustrated spin-glass system. It is possible that such a perturbative expansion turns out to be nonconvergent: If this happens, it may help us to pin down the nonperturbative effects. Motivated by this purpose, we have shown [26] with a two-loop calculation that such an ϵ -expansion can be set up consistently, and that the ordinary RG underlying ideas actually apply also in this case, so that the IR limit of the theory is well defined independently on the regularization technique.

In the present work, we show how the underlying RG ideas emerge in the computation of Ref. [26], and in particular how such a calculation has been performed, so that the reader can fully understand and reproduce it. Moreover, we show by an explicit example of such a computation how the ϵ -expansion could be automatized, i.e., implemented by a computer program, in such a way that high orders of the expansion could be computed to establish its summability properties.

The HEA is defined [23,26] as a system of 2^{k+1} spins, $S_0, \dots, S_{2^{k+1}-1}, S_i = \pm 1$, with an energy function defined

recursively by coupling two systems of 2^k Ising spins

$$H_{k+1}^J[S_0, \dots, S_{2^{k+1}-1}] = H_k^{J_1}[S_0, \dots, S_{2^k-1}] + H_k^{J_2}[S_{2^k}, \dots, S_{2^{k+1}-1}] - \frac{1}{2^{(k+1)\sigma}} \sum_{i < j}^{0, 2^{k+1}-1} J_{12,ij} S_i S_j, \quad (1)$$

where

$$H_1^J[S_1, S_2] = -J2^{-\sigma} S_1 S_2,$$

and all the couplings J_{ij} are Gaussian random variables with zero mean and unit variance. Here σ is a parameter tuning the decay of the interaction strength with distance.

As we will show in the following, the form (1) of the Hamiltonian corresponds to dividing the system in hierarchical embedded blocks of size 2^k , so that the interaction between two spins depends on the distance of the blocks to which they belong [23,24].

The HEA is a hierarchical counterpart of the one-dimensional spin glass with power-law interactions [11], which has received attention recently [27–31].

It is crucial to observe [23] that the sum of the squares of the interaction terms that couple the two subsystems in Eq. (1) scales with k as $2^{2k(1-\sigma)}$. Hence, for $\sigma > 1/2$ the interaction energy scales sub-extensively in the system volume, yielding a non-mean field behavior of the model, while for $\sigma < 1/2$ it grows faster than the volume, and the thermodynamic limit is not defined. On the contrary, for $\sigma > 1$ the interaction energy goes to 0 as $k \rightarrow \infty$, so that no finite-temperature phase transition can occur. Hence, the interesting region we will study is $\sigma \in (1/2, 1)$.

An equivalent definition of the HEA can be given without using the recursion relation (1). Indeed, one can recover Eq. (1) by defining the HEA as a system of 2^k Ising spins with the Hamiltonian,

$$H_k[S] = - \sum_{i,j=0}^{2^k-1} J_{ij} S_i S_j, \quad (2)$$

where J_{ij} are Gaussian random variables with zero mean and variance σ_{ij}^2 . The form of σ_{ij}^2 is given by the following expression: If only the last m digits in the binary representation of the points i and j are different, $\sigma_{ij}^2 = 2^{-2\sigma m}$. This form of the Hamiltonian corresponds to dividing the system in hierarchical embedded blocks of size 2^m , such that the interaction between two spins depends on the distance of the blocks to which they belong. It is important to observe that the quantity σ_{ij}^2 is not translational invariant, but it is invariant under a huge symmetry group, and this will be crucial in the study of the model. The two definitions (1) and (2) are equivalent.

We reproduce the IR behavior of the HEA and calculate its critical exponents by two different methods. Both methods assume the existence of a growing correlation scale length ξ , diverging for $T \rightarrow T_c$ as

$$\xi \propto (T - T_c)^{-\nu},$$

in such a way that for $T \rightarrow T_c$ the theory is invariant under reparametrizations of the length scale.

The first method is analogous to the coarse-graining Wilson's method for the Ising model: The scale-free limit is obtained by imposing invariance with respect to the composition operation of Eq. (1), taking two systems of 2^k spins and yielding a system of 2^{k+1} spins. As for the Dyson ferromagnetic model, thanks to the hierarchical structure of the Hamiltonian, one can obtain closed formulas for physical quantities with respect to such a composition operation, analyze the critical and noncritical fixed points, and extract ν .

The second method is more conventional: The IR divergences appearing for $k \rightarrow \infty$ and $T \rightarrow T_c$ are removed by constructing a renormalized IR-safe theory. The fundamental physical information one extracts from such a renormalized theory is the same as that of the original theory defined by Eq. (1). In particular, the correlation length and its power-law behavior close to the critical point must be the same, and so the critical exponent ν .

The rest of this paper is divided into three main sections: In Sec. II we go through the main steps of the computation with Wilson's method, show that the tensorial operations can be easily implemented diagrammatically, and thus performed by a computer program to compute high orders of the ϵ -expansion. Moreover, we give the two-loop result for ν . In Sec. III the same result is reproduced with the field-theoretical method, and the analogies between the two methods are discussed. In particular, we discuss why Wilson's method would be definitely better than the field-theoretical method for a high-order automatization of the ϵ -expansion. In Secs. II and III, we explicitly do all the steps of the calculation at one loop, giving to the reader all the information needed to reproduce the

two-loop result for ν . Finally, in Sec. IV the two-loop result is discussed in the perspective of the setup of a high-order ϵ -expansion.

II. WILSON'S METHOD

As mentioned before, the hierarchical symmetry structure of the model makes the implementation of a recursive RG equation simple enough to be solved within an approximation scheme. As a matter of fact, let us define the probability distribution of the overlap [1,2],

$$Q_{ab}, \quad a, b = 1, \dots, n$$

$$Q_{ab} = Q_{ba}, \quad Q_{aa} = 0 \quad \forall a, b = 1, \dots, n \quad (3)$$

as

$$Z_k[Q] \equiv \mathbb{E}_J \left[\sum_{\{S_i^a\}_{i,a}} \exp \left(-\beta \sum_{a=1}^n H_k^J [S_0^a, \dots, S_{2^k-1}^a] \right) \right. \\ \left. \times \prod_{a<b=1}^n \delta \left(Q_{ab} - \frac{1}{2^k} \sum_{i=0}^{2^k-1} S_i^a S_i^b \right) \right], \quad (4)$$

where $\beta \equiv 1/T$ is the inverse temperature and \mathbb{E}_J the expectation value with respect to all the couplings $\{J_{12,ij}\}_{ij}$.

It is easy to show that the recursion relation (1) for the Hamiltonian results in a recursion relation for $Z_k[Q]$. Denoting by Tr the trace over the replica indexes, by $\int [dQ]$ the functional integral over $\{Q_{ab}\}_{a<b}$, and setting

$$C \equiv 2^{2(1-\sigma)}, \quad (5)$$

this recursion relation can be derived [23] as follows:

$$Z_k[Q] = \mathbb{E}_J \left\{ \sum_{\{S_i^a\}_{i,a}} \exp \left[-\beta \sum_{a=1}^n \left(H_{k-1}^{J_1} [S_0^a, \dots, S_{2^{k-1}-1}^a] + H_{k-1}^{J_2} [S_{2^{k-1}}^a, \dots, S_{2^k-1}^a] \right) \right. \right. \\ \left. \left. - \frac{1}{2^{k\sigma}} \sum_{i<j}^{0,2^k-1} J_{12,ij} S_i^a S_j^a \right) \right] \prod_{a<b=1}^n \delta \left(Q_{ab} - \frac{1}{2^k} \sum_{i=0}^{2^k-1} S_i^a S_i^b \right) \right\} \\ \times \int [dQ_1 dQ_2] \prod_{a<b=1}^n \left[\delta \left(Q_{1,ab} - \frac{1}{2^{k-1}} \sum_{i=0}^{2^{k-1}-1} S_i^a S_i^b \right) \delta \left(Q_{2,ab} - \frac{1}{2^{k-1}} \sum_{i=2^{k-1}}^{2^k-1} S_i^a S_i^b \right) \right] \\ = \int [dQ_1 dQ_2] \sum_{\{S_i^a\}_{i,a}} \mathbb{E}_{J_1} \left[\exp \left(-\beta \sum_{a=1}^n H_{k-1}^{J_1} [\vec{S}_1^a] \right) \prod_{a<b=1}^n \delta \left(Q_{1,ab} - \frac{1}{2^{k-1}} \sum_{i=0}^{2^{k-1}-1} S_i^a S_i^b \right) \right] \\ \times \mathbb{E}_{J_2} \left[\exp \left(-\beta \sum_{a=1}^n H_{k-1}^{J_2} [\vec{S}_2^a] \right) \prod_{a<b=1}^n \delta \left(Q_{2,ab} - \frac{1}{2^{k-1}} \sum_{i=2^{k-1}}^{2^k-1} S_i^a S_i^b \right) \right] \\ \times \mathbb{E}_{J_{12}} \left[\exp \left(\frac{\beta}{2^{k\sigma}} \sum_{a=1}^n \sum_{i<j}^{0,2^k-1} J_{12,ij} S_i^a S_j^a \right) \right] \prod_{a<b=1}^n \delta \left(Q_{ab} - \frac{Q_{1,ab} + Q_{2,ab}}{2} \right) \\ = \int [dQ_1 dQ_2] \sum_{\{S_i^a\}_{i,a}} \mathbb{E}_{J_1} \left[\exp \left(-\beta \sum_{a=1}^n H_{k-1}^{J_1} [\vec{S}_1^a] \right) \prod_{a<b=1}^n \delta \left(Q_{1,ab} - \frac{1}{2^{k-1}} \sum_{i=0}^{2^{k-1}-1} S_i^a S_i^b \right) \right] \\ \times \mathbb{E}_{J_2} \left[\exp \left(-\beta \sum_{a=1}^n H_{k-1}^{J_2} [\vec{S}_2^a] \right) \prod_{a<b=1}^n \delta \left(Q_{2,ab} - \frac{1}{2^{k-1}} \sum_{i=2^{k-1}}^{2^k-1} S_i^a S_i^b \right) \right]$$

$$\begin{aligned}
 & \times \exp \left[\frac{\beta^2}{42^{2k\sigma}} \sum_{i,j}^{0,2^{k-1}} \left(\sum_{a=1}^n S_i^a S_j^a \right)^2 \right] \prod_{a<b=1}^n \delta \left(Q_{ab} - \frac{Q_{1,ab} + Q_{2,ab}}{2} \right) \\
 & = \int [dQ_1 dQ_2] \sum_{\{S_i^a\}_{i,a}} \mathbb{E}_{J_1} \left[\exp \left(-\beta \sum_{a=1}^n H_{k-1}^{J_1}[\vec{S}_1^a] \right) \prod_{a<b=1}^n \delta \left(Q_{1,ab} - \frac{1}{2^{k-1}} \sum_{i=0}^{2^{k-1}-1} S_i^a S_i^b \right) \right] \\
 & \quad \times \mathbb{E}_{J_2} \left[\exp \left(-\beta \sum_{a=1}^n H_{k-1}^{J_2}[\vec{S}_2^a] \right) \prod_{a<b=1}^n \delta \left(Q_{2,ab} - \frac{1}{2^{k-1}} \sum_{i=2^{k-1}}^{2^k-1} S_i^a S_i^b \right) \right] \\
 & \quad \times \exp \left[\frac{\beta^2}{42^{2k(\sigma-1)}} \sum_{a,b=1}^n \left(\frac{1}{2^k} \sum_i^{0,2^{k-1}} S_i^a S_i^b \right)^2 \right] \prod_{a<b=1}^n \delta \left(Q_{ab} - \frac{Q_{1,ab} + Q_{2,ab}}{2} \right) \\
 & = \exp \left(\frac{\beta^2 C^k}{4} \text{Tr}[Q^2] \right) \int [dQ_1 dQ_2] Z_{k-1}[Q_1] Z_{k-1}[Q_2] \prod_{a<b=1}^n \delta \left(Q_{ab} - \frac{Q_{1,ab} + Q_{2,ab}}{2} \right). \quad (6)
 \end{aligned}$$

The main steps of Eq. (6) can be summarized as follows. We observe first that in the composition operation of Eq. (1), a system 1 of 2^{k-1} spins $\vec{S}_1 \equiv \{S_0, \dots, S_{2^{k-1}-1}\}$ with couplings $J_{1,ij}$ and a system 2 with 2^{k-1} spins $\vec{S}_2 \equiv \{S_{2^{k-1}}, \dots, S_{2^k-1}\}$ and couplings $J_{2,ij}$ are put into interaction with couplings $J_{12,ij}$, and a system with 2^{k+1} spins is obtained. In the first line of Eq. (6) we used Eq. (1) and inserted the integrals over the Q_1, Q_2 that are both equal to 1. In the third line we performed the integral over J_{12} , which is found in the fourth line to depend only on the overlap Q_{ab} . In the fifth line we use the definition (4) of $Z_{k-1}[Q]$, and obtain the equation relating $Z_{k-1}[Q]$ to $Z_k[Q]$. Here and in the rest of this paper, all the Q -independent constants multiplying $Z_k[Q]$ are omitted for simplicity. Equation (6) is analogous to the recursion equation in Dyson's model [15–18], relating the probability distribution $g_k(m)$ of the magnetization at the k -th hierarchical level to $g_{k-1}(m)$. According to the general prescriptions of the replica approach, all the physics of the model is encoded in the $n \rightarrow 0$ limit of $Z_k[Q]$.

We define the rescaled overlap distributions as

$$Z_k[Q] \equiv Z_k[C^{-k/2}Q],$$

and observe that the recursion relation (6) for $Z_k[Q]$ implies a recursion relation for $Z_k[Q]$:

$$\begin{aligned}
 Z_k[Q] & = \exp \left(\frac{\beta^2}{4} \text{Tr}[Q^2] \right) \int [dP] \\
 & \quad \times Z_{k-1} \left[\frac{Q+P}{C^{1/2}} \right] Z_{k-1} \left[\frac{Q-P}{C^{1/2}} \right]. \quad (7)
 \end{aligned}$$

To illustrate the technique used to solve (7) for $Z_k[Q]$, we present our method in a simple toy example, where the matricial field Q_{ab} is replaced by a one-component field ϕ , the functional $Z_k[Q]$ by a function $\Omega_k(\phi)$, and Eq. (7) by

$$\Omega_k(\phi) = \exp \left(\frac{\beta^2}{4} \phi^2 \right) \int d\chi \Omega_{k-1} \left[\frac{\phi + \chi}{C^{1/2}} \right] \Omega_{k-1} \left[\frac{\phi - \chi}{C^{1/2}} \right]. \quad (8)$$

As for Dyson's model, Eq. (8) can be solved by making an ansatz for $\Omega_k(\phi)$. The simplest ansatz for $\Omega_k(\phi)$ is the Gaussian one:

$$\Omega_k(\phi) = \exp[-(d_k \phi^2 + e_k \phi)]. \quad (9)$$

This form corresponds to a mean-field solution. By inserting Eq. (9) into Eq. (8), one finds two recursion equations relating d_k, e_k to d_{k-1}, e_{k-1} :

$$\begin{aligned}
 d_k & = \frac{2d_{k-1}}{C} - \frac{\beta^2}{4}, \\
 e_k & = \frac{2e_{k-1}}{C^{1/2}}.
 \end{aligned}$$

Non-Gaussian solutions can be explicitly constructed perturbatively. Indeed, by setting

$$\Omega_k(\phi) = \exp \left[- \left(d_k \phi^2 + e_k \phi + \frac{u_k}{3} \phi^3 \right) \right], \quad (10)$$

and supposing that u_k is small, one can plug Eq. (10) into Eq. (8) and get

$$\begin{aligned}
 \Omega_k(\phi) & = \exp \left(- \left\{ \left[\frac{2d_{k-1}}{C} - \frac{\beta^2}{4} - \frac{1}{4} \left(\frac{u_{k-1}}{C^{1/2}d_{k-1}} \right)^2 \right] \phi^2 \right. \right. \\
 & \quad + \left(\frac{2e_{k-1}}{C^{1/2}} + \frac{u_{k-1}}{2C^{1/2}d_{k-1}} \right) \phi \\
 & \quad \left. \left. + \frac{1}{3} \left[\frac{2u_{k-1}}{C^{3/2}} + \frac{1}{2} \left(\frac{u_{k-1}}{C^{1/2}d_{k-1}} \right)^3 \right] \phi^3 + O(u_{k-1}^4) \right\} \right), \quad (11)
 \end{aligned}$$

where ϕ -independent constants multiplying $\Omega_k(\phi)$ are omitted for simplicity here and hereinafter. Comparing Eq. (11) with Eq. (10), one finds three recurrence equations relating d_k, e_k, u_k

to $d_{k-1}, e_{k-1}, u_{k-1}$:

$$\begin{aligned} d_k &= \frac{2d_{k-1}}{C} - \frac{\beta^2}{4} - \frac{1}{4} \left(\frac{u_{k-1}}{C^{1/2}d_{k-1}} \right)^2 + O(u_{k-1}^4), \\ e_k &= \frac{2e_{k-1}}{C^{1/2}} + \frac{u_{k-1}}{2C^{1/2}d_{k-1}} + O(u_{k-1}^4), \\ u_k &= \frac{2u_{k-1}}{C^{3/2}} + \frac{1}{2} \left(\frac{u_{k-1}}{C^{1/2}d_{k-1}} \right)^3 + O(u_{k-1}^4). \end{aligned} \quad (12)$$

One can easily analyze the fixed points of the RG-flow equations (12), and the resulting critical properties. We will not enter into these details for the toy model, because all these calculations will be illustrated extensively for the HEA model.

Back to the original problem, Eq. (7) can be solved by making an ansatz for $\mathcal{Z}_k[Q]$, following the same lines as in the toy model case. The simplest form one can suppose for $\mathcal{Z}_k[Q]$ is the Gaussian one:

$$\mathcal{Z}_k[Q] = \exp(-r_k \text{Tr}[Q^2]). \quad (13)$$

This form corresponds to a mean-field solution. By inserting Eq. (13) into Eq. (7), one finds the evolution equation relating r_{k-1} to r_k :

$$r_k = \frac{2r_{k-1}}{C} - \frac{\beta^2}{4}. \quad (14)$$

Corrections to the mean-field solution can be investigated by adding non-Gaussian terms in Eq. (13), which are proportional to higher powers of Q , and consistent with the symmetry properties of the model. It is easy to see [1] that the only cubic term in Q consistent with such symmetry conditions is $\text{Tr}[Q^3]$, so that the non-mean field ansatz of $\mathcal{Z}_k[Q]$ reads

$$\mathcal{Z}_k[Q] = \exp \left[- \left(r_k \text{Tr}[Q^2] + \frac{w_k}{3} \text{Tr}[Q^3] \right) \right]. \quad (15)$$

This correction can be handled by supposing that w_k is small for every k , and performing a systematic expansion in powers of it. By inserting Eq. (15) into Eq. (7), one finds

$$\begin{aligned} \mathcal{Z}_k[Q] &= \exp \left\{ - \left[\left(\frac{2r_{k-1}}{C} - \frac{\beta^2}{4} \right) \text{Tr}[Q^2] + \frac{2w_{k-1}}{3C^{3/2}} \text{Tr}[Q^3] \right] \right\} \\ &\quad \times \int [dP] \exp \left[- S_{k-1}^{(3)}[P, Q] \right], \\ S_{k-1}^{(3)}[P, Q] &\equiv \frac{2r_{k-1}}{C} \text{Tr}[P^2] + \frac{2w_{k-1}}{C^{3/2}} \text{Tr}[QP^2]. \end{aligned} \quad (16)$$

The Gaussian integral in Eq. (16) can be computed exactly. Indeed, defining $\forall a > b$ the super-index $A \equiv (a, b)$, one has

$$\frac{\partial^2 S_{k-1}^{(3)}[P, Q]}{\partial P_A \partial P_B} \equiv \frac{8r_{k-1}}{C} \delta_{AB} + \frac{4w_{k-1}}{C^{3/2}} M_{AB}[Q], \quad (17)$$

where

$$M_{ab,cd}[Q] \equiv N_{ab,cd}[Q] + N_{ab,dc}[Q], \quad (18)$$

$$N_{ab,cd}[Q] \equiv \delta_{bc} Q_{da} + \delta_{ac} Q_{db}. \quad (19)$$

One thus finds

$$\begin{aligned} \mathcal{Z}_k[Q] &= \exp \left\{ - \left[\left(\frac{2r_{k-1}}{C} - \frac{\beta^2}{4} \right) \text{Tr}[Q^2] + \frac{2w_{k-1}}{3C^{3/2}} \text{Tr}[Q^3] \right] \right\} \\ &\quad \times \left[\det \left(\frac{8r_{k-1}}{C} \delta_{AB} + \frac{4w_{k-1}}{C^{3/2}} M_{AB}[Q] \right) \right]^{-\frac{1}{2}}. \end{aligned} \quad (20)$$

The determinant in the right-hand side of Eq. (20) can now be expanded in w_{k-1} . Denoting by Tr the trace over the A -type indexes, it is easy to show that $\text{Tr}[M[Q]] = 0$, and one has to explicitly evaluate the traces $\text{Tr}[M[Q]^2]$, $\text{Tr}[M[Q]^3]$ to expand the determinant to $O(w_{k-1}^3)$. Here we show how the trace $\text{Tr}[M[Q]^2]$ can be evaluated, in order to show to the reader how the tensorial operations over the replica indexes can be generally carried out. By using Eqs. (18) and (19), one has

$$\begin{aligned} \text{Tr}[M[Q]^2] &= \sum_{AB} M[Q]_{AB} M[Q]_{BA} \\ &= \sum_{a>b, c>d} (N_{ab,cd}[Q] + N_{ab,dc}[Q]) \\ &\quad \times (N_{cd,ab}[Q] + N_{cd,ba}[Q]) \\ &= \sum_{a \neq b, c \neq d} N_{ab,cd}[Q] N_{cd,ab}[Q] \\ &= \sum_{a \neq b, c \neq d} (\delta_{bc} Q_{da} + \delta_{ac} Q_{db})(\delta_{da} Q_{bc} + \delta_{ca} Q_{bd}) \\ &= \sum_{a \neq b, c \neq d} \delta_{ca} Q_{bd}^2 \\ &= \sum_{abcd} (1 - \delta_{ab})(1 - \delta_{cd}) \delta_{ca} Q_{bd}^2 \\ &= (n-2) \sum_{ab} Q_{ab}^2 \\ &= (n-2) \text{Tr}[Q^2]. \end{aligned} \quad (21)$$

The steps in Eq. (21) can be summarized as follows: In the second line we write the sums over the super indexes A, B, \dots in terms of the replica indexes a, b, \dots , and in the third line we use the symmetry of $N_{ab,cd}[Q]$ with respect to $a \leftrightarrow b$ and rewrite the sum over $a > b, c > d$ in terms of a sum with $a \neq b, c \neq d$. In the fifth line we find out that just one of the terms stemming from the product $(\delta_{bc} Q_{da} + \delta_{ac} Q_{db})(\delta_{da} Q_{bc} + \delta_{ca} Q_{bd})$ does not vanish, because of the constraints $a \neq b, c \neq d, Q_{aa} = 0$, and because of the Kronecker δ s in the sum. Once we are left with the nonvanishing term, in the sixth line we write explicitly the sum over $a \neq b, c \neq d$ in terms of an unconstrained sum over a, b, c, d by adding the constraints $(1 - \delta_{ab})(1 - \delta_{cd})$. In the seventh line we perform explicitly the sum over the replica indexes, and write everything in terms of the replica-invariant $I_1^{(2)}[Q] \equiv \text{Tr}[Q^2]$ (see Table I).

The trace in Eq. (21) can also be computed with a purely graphical method, which can be easily implemented in a computer program to perform this computation at high orders

TABLE I. Invariants generated at the order $p = 5$. In each line of the table we show the invariants $I_1^{(j)}[Q], \dots, I_{n_j}^{(j)}[Q]$ from left to right.

j	$I_l^{(j)}[Q]$			
2			$\text{Tr}[Q^2]$	
3			$\text{Tr}[Q^3]$	
4	$\text{Tr}[Q^4]$	$\text{Tr}[Q^2]^2$	$\sum_{a \neq c} Q_{ab}^2 Q_{bc}^2$	$\sum_{ab} Q_{ab}^4$
5	$\text{Tr}[Q^5]$	$\text{Tr}[Q^2]\text{Tr}[Q^3]$	$\sum_{abcd} Q_{ab}^2 Q_{bc} Q_{bd} Q_{cd}$	$\sum_{abc} Q_{ab}^3 Q_{ac} Q_{bc}$

in w_k . Let us set

$$\begin{aligned} \mathbf{Tr}_2[f] &\equiv \sum_{a_1 \neq b_1, \dots, a_k \neq b_k} f_{a_1 b_1, \dots, a_k b_k} \\ &= \sum_{a_1 b_1, \dots, a_k b_k} (1 - \delta_{a_1 b_1}) \cdots (1 - \delta_{a_k b_k}) f_{a_1 b_1, \dots, a_k b_k} \end{aligned} \quad (22)$$

for any function of f the replica indexes, and make the graphical identifications shown in Fig. 1. The last line in Eq. (21) can now be reproduced by a purely graphical computation, as shown in Fig. 2. There we show that all the tensorial operations have precise a graphical interpretation, and so that they can be performed without using the cumbersome steps of Eq. (21). This graphical notation is suitable for an implementation in a computer program, which could push our calculation to high orders in w_k . For example, as shown in Fig. 2 in a simple example, while computing $\mathbf{Tr}[M[Q]^k]$ for $k \gg 1$, a proliferation of terms occurs, and some of these terms can be shown to be equal to each other, because they are represented by isomorph graphs, so that the calculation can be extremely simplified.

By following the steps shown in Eq. (21) (or their graphical implementation), all the other tensorial operations can be carried out. In particular, one finds

$$\mathbf{Tr}[M[Q]^3] = (n-2)\text{Tr}[Q^3]. \quad (23)$$

By plugging Eqs. (21) and (23) into Eq. (20), one finds

$$\begin{aligned} \mathcal{Z}_k[Q] &= \exp \left(- \left\{ \left[\frac{2r_{k-1}}{C} - \frac{\beta^2}{4} - \frac{n-2}{4} \left(\frac{w_{k-1}}{2r_{k-1}C^{1/2}} \right)^2 \right] \right. \right. \\ &\quad \times \text{Tr}[Q^2] + \frac{1}{3} \left[\frac{2w_{k-1}}{C^{3/2}} + \frac{n-2}{2} \left(\frac{w_{k-1}}{2r_{k-1}C^{1/2}} \right)^3 \right] \\ &\quad \left. \left. \times \text{Tr}[Q^3] + O(w_{k-1}^4) \right\} \right). \end{aligned} \quad (24)$$

$$\begin{aligned} \delta_{ab} &\equiv a \text{ --- } \bullet \text{ --- } b, \\ Q_{ab} &\equiv a \text{ --- } \blacklozenge \text{ --- } b. \end{aligned}$$

FIG. 1. Graphical identifications representing symbolically the mathematical objects used in tensorial operations. The basic objects are the δ_{ab} function, imposing that the replica indexes a and b are equal (top), and the matrix Q_{ab} (bottom). Once these elements are represented graphically, all the tensorial operations can be worked out by manipulating graphical objects composed by these elementary objects.

Comparing Eq. (24) with Eq. (15), one finds a recursion relation for the coefficients r_k, w_k :

$$\begin{aligned} r_k &= \frac{2r_{k-1}}{C} - \frac{\beta^2}{4} - \frac{n-2}{4} \left(\frac{w_{k-1}}{2C^{1/2}r_{k-1}} \right)^2 + O(w_{k-1}^4), \\ w_k &= \frac{2w_{k-1}}{C^{3/2}} + \frac{n-2}{2} \left(\frac{w_{k-1}}{2C^{1/2}r_{k-1}} \right)^3 + O(w_{k-1}^5). \end{aligned} \quad (25)$$

Setting

$$\epsilon \equiv \sigma - 2/3,$$

Equation (25) shows that if $\epsilon < 0$, $w_k \rightarrow 0$ for $k \rightarrow \infty$, i.e., the corrections to the mean field vanish in the IR limit. In this case, the critical fixed point (r_*, w_*) of Eq. (25) has $w_* = 0$. On the contrary, for $\epsilon > 0$ a nontrivial critical fixed point $w_* \neq 0$ arises. According to general RG arguments, this nontrivial fixed point is proportional to some power of ϵ [12]. In particular, one finds that $w_*^2 = O(\epsilon)$.

The critical exponent ν can be computed [13] by considering the 2×2 matrix \mathcal{M} linearizing the transformation given by Eq. (25) around the critical fixed point (r_*, w_*) ,

$$\begin{pmatrix} r_k - r_* \\ w_k - w_* \end{pmatrix} = \mathcal{M} \cdot \begin{pmatrix} r_{k-1} - r_* \\ w_{k-1} - w_* \end{pmatrix},$$

and is given by

$$\nu = \frac{\log 2}{\log \Lambda}, \quad (26)$$

where Λ is the largest eigenvalue of \mathcal{M} .

Such a procedure can be systematically pushed to higher orders in w_k , and thus in ϵ , by taking into account further corrections to the mean-field solution. Indeed, if we go back to Eq. (20) and consider also the $O(w_{k-1}^4)$ terms on the right-hand side, we find

$$\begin{aligned} &\left[\det \left(\frac{8r_{k-1}}{C} \delta_{AB} + \frac{4w_{k-1}}{C^{3/2}} M_{AB}[Q] \right) \right]^{-\frac{1}{2}} \\ &= \exp \left\{ -\frac{1}{2} \mathbf{Tr} \left[-\frac{1}{2} \left(\frac{w_{k-1}}{2C^{1/2}r_{k-1}} \right)^2 M[Q]^2 \right. \right. \\ &\quad \left. \left. + \frac{1}{3} \left(\frac{w_{k-1}}{2C^{1/2}r_{k-1}} \right)^3 M[Q]^3 - \frac{1}{4} \left(\frac{w_{k-1}}{2C^{1/2}r_{k-1}} \right)^4 \right. \right. \\ &\quad \left. \left. \times M[Q]^4 + O(w_{k-1}^5) \right] \right\}. \end{aligned} \quad (27)$$

By computing explicitly the $O(w_{k-1}^4)$ term on the right-hand side of Eq. (27), one finds

$$\begin{aligned} \text{Tr}[M[Q]^4] &= nI_1^{(4)}[Q] + 3I_2^{(4)}[Q] - 16I_3^{(4)}[Q] - 8I_4^{(4)}[Q], \\ I_1^{(4)}[Q] &\equiv \text{Tr}[Q^4], \\ I_2^{(4)}[Q] &\equiv (\text{Tr}[Q^2])^2, \\ I_3^{(4)}[Q] &\equiv \sum_{b \neq c} Q_{ab}^2 Q_{ac}^2, \\ I_4^{(4)}[Q] &\equiv \sum_{ab} Q_{ab}^4. \end{aligned} \quad (28)$$

Plugging Eq. (28) in Eq. (27) and Eq. (27) in Eq. (20), we see that at $O(w_{k-1}^4)$, Eq. (7) generates the fourth-order monomials $\{I_l^{(4)}[Q]\}_{l=1,\dots,4}$, which are not included into the original ansatz (15). It follows that at $O(w_k^4)$, $\mathcal{Z}_k[Q]$ must be of the form

$$\begin{aligned} \mathcal{Z}_k[Q] &= \exp \left[- \left(r_k \text{Tr}[Q^2] + \frac{w_k}{3} \text{Tr}[Q^3] \right. \right. \\ &\quad \left. \left. + \frac{1}{4} \sum_{l=1}^4 \lambda_{l,k} I_l^{(4)}[Q] \right) \right], \end{aligned} \quad (29)$$

with $\lambda_{l,k} = O(w_k^4) \forall l = 1, \dots, 4$.

By inserting Eq. (29) into Eq. (7) and expanding up to $O(w_{k-1}^4)$, we obtain six recursion equations relating $r_k, w_k, \lambda_{1,k}, \dots, \lambda_{4,k}$ to $r_{k-1}, w_{k-1}, \lambda_{1,k-1}, \dots, \lambda_{4,k-1}$.

Such a systematic expansion can be iterated to any order $O(w_k^p)$, obtaining

$$\mathcal{Z}_k[Q] = \exp \left\{ - \left[c_{1,k}^{(2)} I_1^{(2)}[Q] + \sum_{j=3}^p \frac{1}{j} \sum_{l=1}^{n_j} c_{l,k}^{(j)} I_l^{(j)}[Q] \right] \right\}, \quad (30)$$

where $c_{1,k}^{(2)} \equiv r_k$, $c_{1,k}^{(3)} \equiv w_k$, $c_{l,k}^{(4)} \equiv \lambda_{l,k} \forall l = 1, \dots, 4$, $n_3 = 1$, $n_4 = 4$, and $I_1^{(3)}[Q] \equiv \text{Tr}[Q^3]$. In this way, a recursion equation relating $\{c_{l,k-1}^{(j)}\}_{j,l}$ to $\{c_{l,k}^{(j)}\}_{j,l}$ is obtained.

The number n_j of monomials generated at the step j of this procedure proliferates for increasing j . In Table I we show the invariants $I_l^{(j)}[Q]$ obtained by performing this systematic expansion up to the order $p = 5$. It is interesting to observe that the invariants $\text{Tr}[Q^2]^2, \text{Tr}[Q^2]\text{Tr}[Q^3]$ that are generated, are of $O(n^2)$ if the matrix Q_{ab} is replica symmetric. Notwithstanding this, in general they will give a nonvanishing contribution to the recursion relations $\{c_{l,k-1}^{(j)}\}_{j,l} \rightarrow \{c_{l,k}^{(j)}\}_{j,l}$, and so to ν . The recurrence equations at $O(w_k^5)$ are the following:

$$\begin{aligned} c_{1,k}^{(2)} &= \frac{2c_{1,k-1}^{(2)}}{C} - \frac{\beta^2}{4} - \frac{n-2}{4} \left(\frac{c_{1,k-1}^{(3)}}{2C^{1/2}c_{1,k-1}^{(2)}} \right)^2 + (2n-1) \frac{c_{1,k-1}^{(4)}}{8C c_{1,k-1}^{(2)}} + \frac{c_{2,k-1}^{(4)}}{2C c_{1,k-1}^{(2)}} \left[1 + \frac{n(n-1)}{4} \right] \\ &\quad + (n-2) \frac{c_{3,k-1}^{(4)}}{8C c_{1,k-1}^{(2)}} + \frac{3c_{4,k-1}^{(4)}}{8C c_{1,k-1}^{(2)}} + O[(c_{1,k-1}^{(3)})^6], \end{aligned} \quad (31)$$

$$\begin{aligned} c_{1,k}^{(3)} &= \frac{2c_{1,k-1}^{(3)}}{C^{3/2}} + \frac{n-2}{2} \left(\frac{c_{1,k-1}^{(3)}}{2C^{1/2}c_{1,k-1}^{(2)}} \right)^3 + \frac{3nc_{1,k-1}^{(5)}}{4C^{3/2}c_{1,k-1}^{(2)}} + (n+3) \frac{3c_{2,k-1}^{(5)}}{20C^{3/2}c_{1,k-1}^{(2)}} + \frac{9c_{3,k-1}^{(5)}}{20C^{3/2}c_{1,k-1}^{(2)}} \\ &\quad + \frac{3c_{4,k-1}^{(5)}}{20C^{3/2}c_{1,k-1}^{(2)}} [12 + n(n-1)] - \frac{3c_{1,k-1}^{(3)}}{4C^{1/2}c_{1,k-1}^{(2)}} \left[\frac{(n-1)c_{1,k-1}^{(4)}}{2C c_{1,k-1}^{(2)}} + \frac{2c_{2,k-1}^{(4)}}{C c_{1,k-1}^{(2)}} + \frac{c_{3,k-1}^{(4)}}{2C c_{1,k-1}^{(2)}} \right] + O[(c_{1,k-1}^{(3)})^7], \end{aligned} \quad (32)$$

$$c_{1,k}^{(4)} = \frac{2c_{1,k-1}^{(4)}}{C^2} - \frac{n}{2} \left(\frac{c_{1,k-1}^{(3)}}{2C^{1/2}c_{1,k-1}^{(2)}} \right)^4 + O[(c_{1,k-1}^{(3)})^6], \quad (33)$$

$$c_{4,k}^{(4)} = \frac{2c_{4,k-1}^{(4)}}{C^2} + 4 \left(\frac{c_{1,k-1}^{(3)}}{2C^{1/2}c_{1,k-1}^{(2)}} \right)^4 + O[(c_{1,k-1}^{(3)})^6], \quad (36)$$

$$c_{2,k}^{(4)} = \frac{2c_{2,k-1}^{(4)}}{C^2} - \frac{3}{2} \left(\frac{c_{1,k-1}^{(3)}}{2C^{1/2}c_{1,k-1}^{(2)}} \right)^4 + O[(c_{1,k-1}^{(3)})^6], \quad (34)$$

$$c_{1,k}^{(5)} = \frac{2c_{1,k-1}^{(5)}}{C^{5/2}} + \frac{n+6}{2} \left(\frac{c_{1,k-1}^{(3)}}{2C^{1/2}c_{1,k-1}^{(2)}} \right)^5 + O[(c_{1,k-1}^{(3)})^7], \quad (37)$$

$$c_{3,k}^{(4)} = \frac{2c_{3,k-1}^{(4)}}{C^2} + 8 \left(\frac{c_{1,k-1}^{(3)}}{2C^{1/2}c_{1,k-1}^{(2)}} \right)^4 + O[(c_{1,k-1}^{(3)})^6], \quad (35)$$

$$c_{2,k}^{(5)} = \frac{2c_{2,k-1}^{(5)}}{C^{5/2}} - 40 \left(\frac{c_{1,k-1}^{(3)}}{2C^{1/2}c_{1,k-1}^{(2)}} \right)^5 + O[(c_{1,k-1}^{(3)})^7], \quad (38)$$

Example of a graphical computation

$$\begin{aligned}
 \text{Tr}[M[Q]^2] &= \text{Tr}_2[N[Q]N[Q]] \\
 &= \text{Tr}_2\left[\left(\begin{array}{c} \text{---} \\ \diagup \quad \diagdown \\ \text{---} \end{array} + \begin{array}{c} \text{---} \\ \text{---} \\ \text{---} \end{array}\right)\left(\begin{array}{c} \text{---} \\ \diagup \quad \diagdown \\ \text{---} \end{array} + \begin{array}{c} \text{---} \\ \text{---} \\ \text{---} \end{array}\right)\right] \\
 &= \text{Tr}_2\left[\begin{array}{c} \text{---} \\ \diagup \quad \diagdown \\ \text{---} \\ \diagup \quad \diagdown \\ \text{---} \end{array} + \begin{array}{c} \text{---} \\ \text{---} \\ \text{---} \\ \diagup \quad \diagdown \\ \text{---} \end{array} + \begin{array}{c} \text{---} \\ \diagup \quad \diagdown \\ \text{---} \\ \text{---} \\ \text{---} \end{array} + \begin{array}{c} \text{---} \\ \text{---} \\ \text{---} \\ \text{---} \\ \text{---} \end{array}\right] \\
 &= \text{Tr}_2\left[\begin{array}{c} \text{---} \\ \diagup \quad \diagdown \\ \text{---} \end{array}\right] \\
 &= \begin{array}{c} \text{---} \\ \diagup \quad \diagdown \\ \text{---} \end{array} - \begin{array}{c} \text{---} \\ \text{---} \\ \text{---} \\ \diagup \quad \diagdown \\ \text{---} \end{array} - \begin{array}{c} \text{---} \\ \diagup \quad \diagdown \\ \text{---} \\ \text{---} \\ \text{---} \end{array} + \begin{array}{c} \text{---} \\ \text{---} \\ \text{---} \\ \text{---} \\ \text{---} \end{array} \\
 &= \begin{array}{c} \text{---} \\ \diagup \quad \diagdown \\ \text{---} \end{array} - 2 \times \begin{array}{c} \text{---} \\ \text{---} \\ \text{---} \\ \diagup \quad \diagdown \\ \text{---} \end{array} \\
 &= n \times \begin{array}{c} \text{---} \\ \diagup \quad \diagdown \\ \text{---} \end{array} - 2 \times \begin{array}{c} \text{---} \\ \text{---} \\ \text{---} \\ \diagup \quad \diagdown \\ \text{---} \end{array} \\
 &= (n-2)\text{Tr}[Q^2]
 \end{aligned}$$

FIG. 2. Graphical computation of $\text{Tr}[M[Q]^2]$ in Eq. (21). In the second line, the two addends of the matrix $N[Q]_{ab,cd}$ in Eq. (19) are represented graphically in terms of the graphical objects defined in Fig. 1. In the third line, the legs of such addends are contracted with each other, and four terms are generated. The second and the third term can be easily recognized to be topologically identical, and so equal. According to the condition $Q_{aa} = 0$ in Eq. (3), the first term in the third line vanishes. Indeed, in this term the lines coming out of the square vertex Q_{ab} are connected by a circuit, meaning that the matrix element Q_{ab} is computed with $a = b$, and thus vanishes. The second and third terms in the third line also vanish because, according to Eq. (22), the dummy indexes in Tr_2 must satisfy $a_1 \neq b_1, a_2 \neq b_2$, while the graphical structure of the second and third terms enforces the constraint $a_2 = b_2, a_1 = b_1$ respectively. Moreover, the two top lines in the third term are actually equivalent to just one line, because of the relation $\delta_{ab}^2 = \delta_{ab}$. Hence, we are left with a single term in the fourth line. In the fifth line, we perform graphically the operation Tr_2 . Such an operation can be easily implemented graphically by looking at the second line of Eq. (22). Let us expand the product of δ s in the second line of Eq. (22), and recall from Fig. 1 that δ_{ab} represents a line with a circular dot connecting a with b . Hence, given a graphical object O with external legs (indexes) $(a_1, b_1), \dots, (a_k, b_k)$, $\text{Tr}_2[O]$ is nothing but the sum of all the possible 2^k contractions (performed with a line with a circular dot) of these external legs, where each contracted term is multiplied by $(-1)^{\#\text{of contractions of the term}}$. In this case $k = 2$, so we generate 2^2 terms in the fifth line. In the sixth line, we take into account the fact that the second and third terms in the fifth line are topologically isomorph, and that the fourth term in the fifth line vanishes because of the condition $Q_{aa} = 0$. In the seventh line the unconstrained sum over the replica indexes is finally performed. This can be done graphically in the following way: When we have an external line connected to a round vertex, summing over the replica index represented by that line means that one has to simply remove the line (this is the graphical implementation of the relation $\sum_b \delta_{ab} g_b = g_a$). We do this in the first term: We sum over the top-left index, and remove the line on the top. Then we sum over the top-right index by simply multiplying by n . The sum over the bottom-left and bottom-right indexes simply yields $\text{Tr}[Q^2]$. We do the same for the second term: We sum over the top-right index and remove the top line, then sum over the top-left index and remove the top-left line. Then, the sum over the bottom-left and bottom-right indexes yields $\text{Tr}[Q^2]$. Hence, we get the same result as in Eq. (21).

$$c_{3,k}^{(5)} = \frac{2c_{3,k-1}^{(5)}}{C^{5/2}} + 30 \left(\frac{c_{1,k-1}^{(3)}}{2C^{1/2}c_{1,k-1}^{(2)}} \right)^5 + O[(c_{1,k-1}^{(3)})^7], \quad (39)$$

$$c_{4,k}^{(5)} = \frac{2c_{4,k-1}^{(5)}}{C^{5/2}} + 5 \left(\frac{c_{1,k-1}^{(3)}}{2C^{1/2}c_{1,k-1}^{(2)}} \right)^5 + O[(c_{1,k-1}^{(3)})^7]. \quad (40)$$

By looking at Eqs. (33)–(40) and using the definition (5), it is easy to see that the coefficients $c_{l,k}^{(4)}, c_{l,k}^{(5)}$ scale to zero as $k \rightarrow \infty$ if $\epsilon < 1/12$. It is easy to find out that this is actually true for all the coefficients $c_{l,k}^{(j)}$ with $j > 3$. Such a critical value $\epsilon = 1/12$ will be reproduced also in the field-theoretical approach in Sec. III.

The evolution Eqs. (31)–(40) depend smoothly on the replica number n , so that the analytical continuation $n \rightarrow 0$, can be done directly. By linearizing the transformation (31)–(40) around the critical fixed point $\{c_{l,*}^{(j)}\}_{j,l}$ and computing the matrix \mathcal{M} , one can extract Λ , and so ν for $n = 0$ to the order ϵ^2 by using Eq. (26). We find

$$\begin{aligned} \nu &= 3 + 36\epsilon + [432 - 27(50 + 55 \times 2^{1/3}) \\ &\quad + 53 \times 2^{2/3}] \log 2 \epsilon^2 + O(\epsilon^3). \end{aligned} \quad (41)$$

At order ϵ , our result for ν is the same as that of the power-law interaction spin glass [11] [where $\epsilon \equiv 3(\sigma - 2/3)$]. Notwithstanding this, the coefficients of the expansion in these two models will be in general different at two or more loops. As a matter of fact, the binary-tree interaction structure of the HEA emerges in the nontrivial $\log 2, 2^{1/3}$ factors in the coefficient of ϵ^2 in Eq. (41), which cannot be there in the power-law case.

Before discussing the result in Eq. (41), we point out that Wilson's method explicitly implements the binary-tree structure of the model when approaching the IR limit. As a matter of fact, the hierarchical structure of the model is explicitly exploited to construct the steps of the RG transformation. Nevertheless, if the IR limit is unique and well defined, physical observables such as ν must not depend on the technique we use to compute them in such a limit. It is thus important to verify that Eq. (41) does not depend on the method we used to reproduce the IR behavior of the theory. This has been done by reproducing Eq. (41) with a quite different field-theoretical approach.

III. FIELD-THEORETICAL METHOD

Here the IR limit is performed by constructing a functional integral field theory and by removing its IR divergences within the minimal subtraction scheme.

While in Wilson's method the IR limit was performed by looking at the scale-invariant fixed points for $k \rightarrow \infty$ after solving the recursion relation (7), in this case we perform before the large- k limit, remove the resulting IR singularities through re-normalization, and then perform the scale-invariant (IR) limit by means of the Callan-Symanzik equation.

This computation is better performed by slightly changing the definition of the model. Indeed, the following redefinition of the interaction term in Eq. (1),

$$\sum_{i<j}^{0,2^{k+1}-1} J_{12,ij} S_i S_j \rightarrow \sum_{i=0}^{2^k-1} \sum_{j=2^k}^{2^{k+1}-1} J_{12,ij} S_i S_j \quad (42)$$

is equivalent to the original definition (1) and makes the field-theory computations simpler. The equivalence of Eq. (42) with the original definition (1) can be shown [23] by observing that the scaling of the spin coupling in the model defined by Eq. (42) differs from that in Eq. (1) for a constant multiplicative factor, and thus that the two options are equivalent, and must yield the same critical exponents. Notwithstanding this, the critical temperature of the model defined by Eq. (1) and that of the model defined by Eq. (42) are different. This can be verified by considering how the recursion relation (6) is modified when one applies the redefinition (42).

The only difference is the third factor in the second line of Eq. (6), which is now given by

$$\begin{aligned} \mathbb{E}_{J_{12}} \left[\exp \left(\frac{\beta}{2^{k\sigma}} \sum_{a=1}^n \sum_{i=0}^{2^{k-1}-1} \sum_{j=2^{k-1}}^{2^k-1} J_{12,ij} S_i^a S_j^a \right) \right] \\ = \exp \left\{ \frac{\beta^2 C^k}{4} \left[\text{Tr}[Q^2] - \frac{1}{4} (\text{Tr}[Q_1^2] + \text{Tr}[Q_2^2]) \right] \right\}. \end{aligned}$$

It follows that the recursion relation (6) becomes

$$\begin{aligned} Z_k[Q] &= \exp \left(\frac{\beta^2 C^k}{4} \text{Tr}[Q^2] \right) \int [dQ_1 dQ_2] \\ &\times \exp \left(-\frac{\beta^2 C^k}{16} \text{Tr}[Q_1^2] \right) Z_{k-1}[Q_1] \\ &\times \exp \left(-\frac{\beta^2 C^k}{16} \text{Tr}[Q_2^2] \right) Z_{k-1}[Q_2] \\ &\times \prod_{a<b=1}^n \delta \left(Q_{ab} - \frac{Q_{1,ab} + Q_{2,ab}}{2} \right). \quad (43) \end{aligned}$$

Setting

$$\mathcal{X}_k[Q] \equiv \exp \left(-\frac{\beta^2 C}{16} \text{Tr}[Q^2] \right) Z_k[C^{-k/2} Q],$$

one can rewrite Eq. (43) as

$$\begin{aligned} \mathcal{X}_k[Q] &= \exp \left[\frac{\beta^2}{4} \left(1 - \frac{C}{4} \right) \text{Tr}[Q^2] \right] \int [dP] \\ &\times \mathcal{X}_{k-1} \left(\frac{Q+P}{C^{1/2}} \right) \mathcal{X}_{k-1} \left(\frac{Q-P}{C^{1/2}} \right). \quad (44) \end{aligned}$$

By comparing Eq. (44) with Eq. (7), it is finally clear that the redefinition (42) results in an effective redefinition of the inverse temperature β .

The redefinition (42) also has a clear physical meaning. Indeed, the original definition (1) is such that, when two subsystems of 2^k spins are coupled to form a system with 2^{k+1} spins, one introduces couplings $J_{12,ij}$ between the two subsystems and between the spins within each subsystem, while in Eq. (42) only couplings between the two subsystems are introduced.

By iterating the recursion relation (1), one has an explicit form for the Hamiltonian $H_k^J[\vec{S}]$ of a system of 2^k spins in the large- k limit. Then, the average of the replicated partition function is expressed as an integral over the local overlap field $Q_{iab} \equiv S_i^a S_i^b$:

$$\begin{aligned} \mathbb{E}_J[Z^n] &= \mathbb{E}_J \left[\sum_{\{S_i^a\}_{i,a}} \exp \left(-\beta \sum_{a=1}^n H_k^J[S_0^a, \dots, S_{2^k-1}^a] \right) \right] \\ &= \int [dQ] e^{-S[Q]}. \end{aligned}$$

By using a dimensional analysis, it is easy to pick up the terms in $S[Q]$ that are relevant in the IR limit. It is easy to check that $S[Q]$ is given by the sum of a quadratic term in Q_{iab} , plus a cubic term, plus higher-degree terms. The dimensions of the field Q_{iab} can be computed by imposing the adimensionality of the quadratic term, and so the dimensions of the coefficient g of the cubic term and of those of the higher-degree terms. One finds that the dimensions of g in energy is $[g] = 3\epsilon$. Thus, as in Wilson's method, the cubic term scales to zero in the IR limit for $\epsilon < 0$, while a nontrivial fixed point appears for $\epsilon > 0$. As in Wilson's method, it is easy to see that for $\epsilon < 1/12$ all the higher-degree terms in $S[Q]$ scale to zero in the IR limit. Thus, the IR-dominant part of the action reads

$$S[Q] = \frac{1}{2} \sum_{i,j=0}^{2^k-1} \Delta_{ij} \text{Tr}[Q_i Q_j] + \frac{g}{3!} \sum_{i=0}^{2^k-1} \text{Tr}[Q_i^3]. \quad (45)$$

In the derivation of Eq. (45), the bare propagator Δ_{ij} originally depends on i, j through the difference $\mathcal{I}(i) - \mathcal{I}(j)$, where the function $\mathcal{I}(i)$ is defined as follows: Given $i \in [0, 2^k - 1]$ and its expression in base 2,

$$i = \sum_{j=0}^{k-1} a_j 2^j, \quad \mathcal{I}(i) \equiv \sum_{j=0}^{k-1} a_{k-1-j} 2^j. \quad (46)$$

Hence, the quadratic term of Eq. (45) is not invariant under spatial translations. This would make any explicit computation of the loop integrals, and so of the critical exponents, extremely difficult to perform. This problem can be overcome by a relabeling of the sites of the lattice [33],

$$\mathcal{I}(i) \rightarrow i, \forall i = 0, \dots, 2^k - 1.$$

After relabeling one obtains that Δ_{ij} depends on i, j just through the difference $i - j$, thus $S[Q]$ is translationally invariant, and the ordinary Fourier transform techniques [33,34] can be employed. In particular, the Fourier representation of the propagator is

$$\Delta_{ij} = \frac{1}{2^k} \sum_{p=0}^{2^k-1} \exp \left[\frac{-2\pi i p(i-j)}{2^k} \right] (|p|_2^{2\sigma-1} + m), \quad (47)$$

where $|p|_2$ is the diadic norm of p [32], and the mass $m \propto T - T_c$ has dimensions $[m] = 2\sigma - 1$.

An interesting feature of the action (45) is the fact the propagator Δ in Eq. (47) depends on the momentum p through its diadic norm $|p|_2$. If we look at the original derivation of the recursion RG equation for the Ising model in finite dimension (in particular, to the Polyakov derivation [13]), we find that the

basic approximation was to introduce an ultrametric structure in momentum space: The momentum space is divided in shells, and the sum of two momenta of a given shell cannot give a momentum of a higher momentum scale cell. This has a nice similarity with the metric properties of the diadic norm, where if p_1, p_2 are two integers, their diadic norms satisfy [32] $|p_1 + p_2|_2 \leq \max(|p_1|_2, |p_2|_2)$.

The field theory defined by Eq. (45) reproduces the $\text{Tr}[Q^3]$ interaction term of the well-know effective actions describing the spin-glass transition in short-range [35] and long-range [11,36] spin glasses. Notwithstanding this similarity, the novelty of the HEA is that a high-order ϵ -expansion can be quite easily automatized within Wilson's method, by means of a symbolic manipulation program solving the simple RG equation (7). This is not true for such short- and long-range [11,35,36] models, where the only approach to compute the exponents is the field-theoretical one. Indeed, to the best of our knowledge, nobody ever managed to automatize a high-order computation of the critical exponents within the field-theoretical minimal subtraction scheme, even for the Ising model, because such an automation is not an easy task [37].

The field theory defined by Eq. (45) can be now analyzed within the loop-expansion framework. The renormalized mass and coupling constant are defined as

$$m = m_r + \delta m, \tag{48}$$

$$g = m_r^{\frac{3\epsilon}{2\sigma-1}} g_r Z_g. \tag{49}$$

We define the one-particle-irreducible [12] (1PI) renormalized correlation functions $\Gamma_r^{(m,l)}$ in terms of the bare 1PI correlation functions $\Gamma^{(m,l)}$ as

$$\begin{aligned} \Gamma_r^{(m,l)}(a_1 b_1 i_1 \cdots a_m b_m i_m; j_1 \cdots j_l; g_r, m_r^{\frac{1}{2\sigma-1}}) \\ \equiv Z_2^l \Gamma^{(m,l)}(a_1 b_1 i_1 \cdots a_m b_m i_m; j_1 \cdots j_l; g, m^{\frac{1}{2\sigma-1}}). \end{aligned}$$

Since this model has long-range interactions, the field Q_{ab} is not renormalized, and [12] $Z_Q = 1$. Hence, all we need to compute ν are [12] the renormalization constants Z_g, Z_2 and δm . These can be obtained by computing the IR-divergent parts of $\Gamma_r^{(3,0)}, \Gamma_r^{(2,1)}$ with the minimal subtraction scheme [12]. In other words, one takes the IR limit $m_r \rightarrow 0$, and systematically removes the resulting ϵ -singular parts of the correlations functions by absorbing them into the renormalization constants Z_g, Z_2 .

The Feynman diagrams contributing to $\Gamma_r^{(2,1)}, \Gamma_r^{(3,0)}$ are shown in Figs. 3 and 4, respectively, and their singular parts are in the form of $1/\epsilon, 1/\epsilon^2$ poles.

Here we show by a simple example how the ϵ -divergent part of such diagrams can be computed. Let us consider the one-loop expansion of $\Gamma_r^{(3,0)}$. This is obtained by picking up the $\text{Tr}[Q^3]$ term in the renormalized 1PI generating functional [12]:

$$\begin{aligned} \Gamma_r[Q] = \frac{1}{2} \sum_{i,j=0}^{2^k-1} \Delta_{ij} \text{Tr}[Q_i Q_j] + \frac{m_r^{3\epsilon} g_r}{3!} \sum_{i=0}^{2^k-1} \text{Tr}[Q_i^3] \\ \times \left(Z_g + \frac{n-2}{8} m_r^{\frac{6\epsilon}{2\sigma-1}} \mathcal{I}_7 g_r^2 \right) + O(g_r^5). \end{aligned} \tag{50}$$

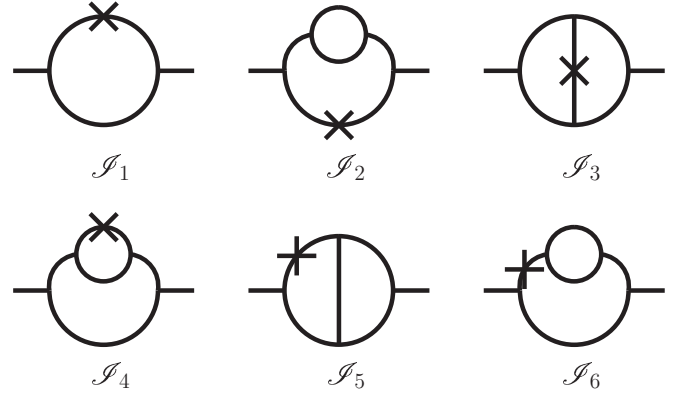


FIG. 3. One- and two-loop Feynman diagrams contributing to $\Gamma_r^{(2,1)}$. The crosses represent $\text{Tr}[Q^2]$ insertions. From left to right, such diagrams computed at zero external momenta are equal to $\mathcal{I}_1, \mathcal{I}_2, \mathcal{I}_3, \mathcal{I}_4, \mathcal{I}_5, \mathcal{I}_6$, respectively.

The loop integral,

$$\mathcal{I}_7 \equiv \frac{1}{2^k} \sum_{p=0}^{2^k-1} \frac{1}{(m_r + \delta m + |p|_2^{2\sigma-1})^3}, \tag{51}$$

is represented by the first diagram in Fig. 4.

Equation (51) has a well-defined limit for $k \rightarrow \infty$. Indeed, thanks to the translational invariance of the theory, the argument of the sum on the right-hand side of Eq. (51) depends on p just through its diadic norm. It follows that the sum \mathcal{I}_7 can be transformed into a sum over all possible values of $|p|_2$. Indeed, using the standard result [32] that the number of integers $p \in [0, 2^k - 1]$ such that $|p|_2 = 2^{-j}$, i.e., the volume of the diadic shell, is given by 2^{-j+k-1} , Eq. (51) becomes

$$\begin{aligned} \mathcal{I}_7 = \sum_{j=0}^{k-1} 2^{-j-1} \frac{1}{[m_r + \delta m + 2^{-j(2\sigma-1)}]^3} \\ \rightarrow \sum_{j=0}^{\infty} 2^{-j-1} \frac{1}{[m_r + \delta m + 2^{-j(2\sigma-1)}]^3}, \end{aligned} \tag{52}$$

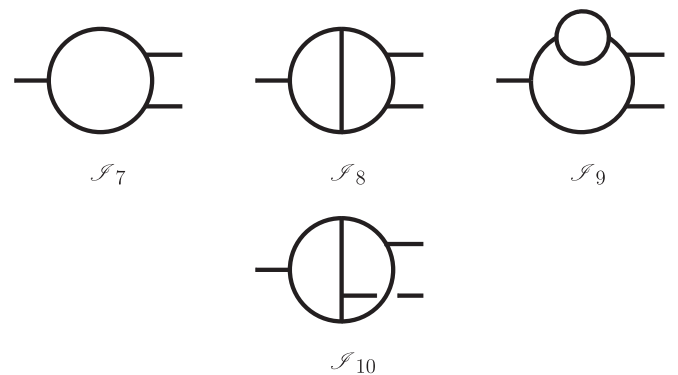


FIG. 4. One- and two-loop Feynman diagrams contributing to $\Gamma_r^{(3,0)}$. From left to right, such diagrams computed at zero external momenta are equal to $\mathcal{I}_7, \mathcal{I}_8, \mathcal{I}_9, \mathcal{I}_{10}$, respectively. The last diagram is nonplanar.

where in the second line of Eq. (52) the $k \rightarrow \infty$ limit has been taken, because the sum in the first line is convergent. By using the fact that $\delta m = O(g_r^2)$, we can rewrite Eq. (52) as

$$\mathcal{I}_7 = \sum_{j=0}^{\infty} 2^{-j-1} \frac{1}{[m_r + 2^{-j(2\sigma-1)}]^3} + O(g_r^2). \quad (53)$$

It is easy to see that \mathcal{I}_7 is IR divergent for $m_r \rightarrow 0$. Indeed, in the limit $m_r \rightarrow 0$ the sum over j in Eq. (53) is dominated by the terms in the IR region $2^{-j} = |p|_2 \rightarrow 0$. The j s corresponding to this region go to infinity as $m_r \rightarrow 0$, yielding a divergent sum in \mathcal{I}_7 .

In the IR region, the sum on the right-hand side of Eq. (53) can be approximated by an integral, because the integrand function is almost constant in the interval $[j, j+1]$ for large j . Setting $q \equiv 2^{-j}$, for $m_r \rightarrow 0$ we have $-q \log 2 dj = dq$, and

$$\begin{aligned} \mathcal{I}_7 &= \frac{1}{2 \log 2} \int_0^1 \frac{dq}{[m_r + q^{2\sigma-1}]^3} + O(g_r^2) \\ &= \frac{m_r^{-\frac{6\epsilon}{2\sigma-1}}}{2 \log 2} \int_0^{m_r^{-\frac{1}{2\sigma-1}}} \frac{dx}{(1+x^{2\sigma-1})^3} + O(g_r^2) \\ &\rightarrow \frac{m_r^{-\frac{6\epsilon}{2\sigma-1}}}{2 \log 2} \int_0^{\infty} \frac{dx}{(1+x^{2\sigma-1})^3} + O(g_r^2). \end{aligned} \quad (54)$$

The integral on the right-hand side of the last line in Eq. (54) is convergent for $\epsilon > 0$, and diverges as $\epsilon \rightarrow 0$. Its ϵ -divergent part can be easily evaluated,

$$\begin{aligned} \mathcal{I}_7 &= \frac{m_r^{-\frac{6\epsilon}{2\sigma-1}}}{4 \log 2} \Gamma\left(3 + \frac{1}{1-2\sigma}\right) \\ &\quad \times \Gamma\left(1 + \frac{1}{1-2\sigma}\right) + O(g_r^2) \\ &= m_r^{-\frac{6\epsilon}{2\sigma-1}} \left[\frac{1}{12\epsilon \log 2} + O_\epsilon(1) \right] + O(g_r^2), \end{aligned} \quad (55)$$

where Γ is the Euler-gamma function and $O_\epsilon(1)$ denotes terms that stay finite as $\epsilon \rightarrow 0$. As we will show in the following, these finite terms give a contribution to the renormalization constants at two loops. By plugging Eq. (55) into Eq. (50), one can compute the g_r^2 coefficient of Z_g by imposing that the ϵ -singular part of \mathcal{I}_7 is canceled by Z_g . For $n=0$ we have

$$Z_g = 1 + \frac{1}{48\epsilon \log 2} g_r^2 + O(g_r^4). \quad (56)$$

By repeating the same computation for the generating functional $\Gamma_r[Q, K]$ of correlation functions with $\text{Tr}[Q^2]$ insertions and imposing that the $\sum_{i=0}^{2^k-1} K_i Q_i^2$ term is finite, i.e., that $\Gamma_r^{(2,1)}$ is finite, we obtain

$$Z_2 = 1 + \frac{1}{24\epsilon \log 2} g_r^2 + O(g_r^4).$$

Such a procedure has been pushed at two loops by an explicit calculation. Even if the evaluation of the ϵ -divergent part of the two-loop diagrams is more involved, the techniques and underlying ideas are exactly the same as those used to compute the one-loop diagram \mathcal{I}_7 . In Figs. 3 and 4 we show the Feynman diagrams contributing to the finiteness conditions of $\Gamma_r^{(2,1)}$ and of $\Gamma_r^{(3,0)}$, respectively. We denote by $\mathcal{I}_7, \dots, \mathcal{I}_6$ the diagrams in Fig. 3 evaluated at zero external momenta, and by $\mathcal{I}_7, \dots, \mathcal{I}_{10}$ those in Fig. 4 evaluated at zero momenta. It is easy to show that the equalities

$$\begin{aligned} \mathcal{I}_7 &= \mathcal{I}_7, \\ \mathcal{I}_2 &= \mathcal{I}_6 = \mathcal{I}_9, \\ \mathcal{I}_3 &= \mathcal{I}_{10}, \\ \mathcal{I}_4 &= \mathcal{I}_5 = \mathcal{I}_8 \end{aligned}$$

hold, and so that all we need to compute the renormalization constants are $\mathcal{I}_7, \mathcal{I}_2, \mathcal{I}_3, \mathcal{I}_4$. \mathcal{I}_7 is given by Eq. (51), while the other loop integrals are

$$\begin{aligned} \mathcal{I}_2 &= \frac{1}{2^{2k}} \sum_{p=0}^{2^k-1} \sum_{q=0}^{2^k-1} \frac{1}{(m_r + \delta m + |p|_2^{2\sigma-1})^4 (m_r + \delta m + |q|_2^{2\sigma-1}) (m_r + \delta m + |p-q|_2^{2\sigma-1})}, \\ \mathcal{I}_3 &= \frac{1}{2^{2k}} \sum_{p=0}^{2^k-1} \sum_{q=0}^{2^k-1} \frac{1}{(m_r + \delta m + |p|_2^{2\sigma-1})^2 (m_r + \delta m + |q|_2^{2\sigma-1})^2 (m_r + \delta m + |p-q|_2^{2\sigma-1})^2}, \\ \mathcal{I}_4 &= \frac{1}{2^{2k}} \sum_{p=0}^{2^k-1} \sum_{q=0}^{2^k-1} \frac{1}{(m_r + \delta m + |p|_2^{2\sigma-1})^3 (m_r + \delta m + |q|_2^{2\sigma-1})^2 (m_r + \delta m + |p-q|_2^{2\sigma-1})}. \end{aligned}$$

In the limit $m_r \rightarrow 0$, $\mathcal{I}_2, \mathcal{I}_3, \mathcal{I}_4$ are given by

$$\begin{aligned} \mathcal{I}_2 &= m_r^{-\frac{12\epsilon}{2\sigma-1}} \left[\left(\frac{2}{2^{2/3}-1} - \frac{1}{2^{1/3}-1} - 1 \right) \frac{1}{48\epsilon \log 2} \right] + O_\epsilon(1) + O(g_r^2), \\ \mathcal{I}_3 &= m_r^{-\frac{12\epsilon}{2\sigma-1}} \left(\frac{1}{2^{1/3}-1} \frac{1}{16\epsilon \log 2} \right) + O_\epsilon(1) + O(g_r^2), \end{aligned}$$

$$\mathcal{S}_4 = m_r^{-\frac{12\epsilon}{2\sigma-1}} \left\{ \frac{1}{2} \left[\frac{1}{(12\epsilon \log 2)^2} - \left(\frac{3}{8(\log 2)^2} + \frac{1}{48 \log 2} \right) \frac{1}{\epsilon} \right] + \left(\frac{1}{2^{1/3} - 1} + \frac{1}{2^{2/3} - 1} \right) \frac{1}{48\epsilon \log 2} \right\} + O_\epsilon(1) + O(g_r^2).$$

The finiteness of $\Gamma_r^{(3,0)}$ is imposed by making finite the $\sum_{i=0}^{2^k-1} \text{Tr}[Q_i^3]$ term in the 1PI generating functional $\Gamma_r[Q]$. The finiteness of $\Gamma_r^{(2,1)}$ is imposed by making finite the $\sum_{i=0}^{2^k-1} K_i Q_i^2$ term in the 1PI generating functional $\Gamma_r[Q, K]$. The two-loop expansion of $\Gamma_r[Q]$ and of $\Gamma_r[Q, K]$ read

$$\begin{aligned} \Gamma_r[Q] = & g_r \sum_{i=0}^{2^k-1} \text{Tr}[Q_i^3] \left\{ \frac{m_r^{\frac{3\epsilon}{2\sigma-1}} Z_g}{3!} + \frac{g_r^2(n-2)}{6} \left(\frac{m_r^{\frac{3\epsilon}{2\sigma-1}} Z_g}{2} \right)^3 \mathcal{S}_7 \right. \\ & \left. + \frac{g_r^4 m_r^{\frac{15\epsilon}{2\sigma-1}} Z_g^5}{3!2^7} [6(n-2)^2 \mathcal{S}_9 + 6(n-2)^2 \mathcal{S}_8 + 2(n(n-1) - 4 - (n-2)^2) \mathcal{S}_{10}] + O(g_r^6) \right\} \\ & + \dots, \end{aligned} \quad (57)$$

$$\begin{aligned} \Gamma_r[Q, K] = & \sum_{i=0}^{2^k-1} K_i \text{Tr}[Q_i^2] \left\{ \frac{Z_2}{4} + \frac{g_r^2 Z_2 Z_g^2 m_r^{\frac{6\epsilon}{2\sigma-1}} (n-2)}{16} \mathcal{S}_1 + \frac{g_r^4 m_r^{\frac{12\epsilon}{2\sigma-1}} (n-2)^2}{2^8} [2(3\mathcal{S}_2 + 2\mathcal{S}_4) \right. \\ & \left. + 4\mathcal{S}_5 + \mathcal{S}_3] + O(g_r^6) \right\} + \dots, \end{aligned} \quad (58)$$

where the \dots in Eq. (57) stands for terms that are not cubic in Q_i , while the \dots in Eq. (58) stands for terms that are not quadratic in Q_i and linear in K_i . The renormalization constants Z_g, Z_2 are calculated by imposing that the renormalized correlation functions $\Gamma_r^{(3,0)}, \Gamma_r^{(2,1)}$ are finite, i.e., that the term in curly brackets in Eq. (57) and that in Eq. (58) have no singularities [12] in ϵ . At this purpose, we observe that the finite part of the integral \mathcal{S}_7 contributes to the renormalization constants at two loops. For example, let us consider the second addend in curly brackets on the right-hand side of Eq. (57). By using Eq. (55) and the one-loop result (56) for Z_g , it is easy to see that this term produces an ϵ -divergent term, given by

$$\frac{g_r^2(n-2)}{48} m_r^{\frac{9\epsilon}{2\sigma-1}} \frac{3}{48\epsilon \log 2} g_r^2 O_\epsilon(1), \quad (59)$$

where $O_\epsilon(1)$ is the finite part of \mathcal{S}_7 in Eq. (55). The term in Eq. (59) is of $O(g_r^4)$ and singular in ϵ . Hence, it contributes to the $O(g_r^4)$ term in Z_g .

After setting $n = 0$ and imposing the finiteness conditions, we find

$$\begin{aligned} Z_g = & 1 + \frac{g_r^2}{48\epsilon \log 2} \\ & + g_r^4 \left[\frac{1}{1536\epsilon^2 (\log 2)^2} + \frac{5 + 2 \times 2^{2/3}}{512\epsilon \log 2} \right] + O(g_r^6), \end{aligned} \quad (60)$$

$$\begin{aligned} Z_2 = & 1 + \frac{g_r^2}{24\epsilon \log 2} \\ & + g_r^4 \left[\frac{1}{576\epsilon^2 (\log 2)^2} - 5 \frac{(1 + 11 \times 2^{1/3} + 7 \times 2^{2/3})}{2304\epsilon \log 2} \right] \\ & + O(g_r^6). \end{aligned} \quad (61)$$

It is also easy to verify that $\delta m = O(g_r^4)$.

Once the IR-safe renormalized theory has been constructed, the effective coupling constant $g(\lambda)$ at the energy scale λ is computed from the Callan-Symanzik equation in terms of the β function by setting $\mu \equiv m_r^{\frac{1}{2\sigma-1}}$,

$$\beta(g_r) = \mu \frac{\partial g_r}{\partial \mu} \Big|_{g,m}, \quad \beta(g(\lambda)) = \lambda \frac{dg(\lambda)}{d\lambda}. \quad (62)$$

$\beta(g_r)$ can be explicitly computed in terms of the renormalization constant Z_g by applying $\mu \frac{\partial}{\partial \mu} \Big|_{g,m}$ on both sides of Eq. (49):

$$0 = \mu \frac{\partial}{\partial \mu} \Big|_{g,m} (\mu^{3\epsilon} g_r Z_g). \quad (63)$$

The right-hand side of Eq. (63) can then be worked out explicitly by using the two-loop result (60) and substituting systematically $\beta(g_r)$ to $\mu \frac{\partial g_r}{\partial \mu} \Big|_{g,m}$. In this way, an explicit equation for $\beta(g_r)$ is obtained. One finds

$$\beta(g_r) = -3\epsilon g_r + \frac{g_r^3}{8 \log 2} + 3 \frac{5 + 2 \times 2^{2/3}}{128 \log 2} g_r^5 + O(g_r^7). \quad (64)$$

Setting $g_r^* \equiv g(\lambda = 0)$, we see from Eq. (64) that the fixed point $g_r^* = 0$ is stable only for $\epsilon < 0$, while for $\epsilon > 0$ a non-Gaussian fixed point g_r^* of order $\sqrt{\epsilon}$ arises, as predicted by dimensional considerations and by Wilson's method. Now the IR limit $\lambda \rightarrow 0$ can be safely taken, and the scaling relations yield ν , in terms of g_r^* and Z_2 ,

$$\eta_2[g_r] \equiv \mu \frac{\partial \log Z_2}{\partial \mu} \Big|_{g,m}, \quad \nu = \frac{1}{\eta_2[g_r^*] + 2\sigma - 1}. \quad (65)$$

By plugging the two-loop result for g_r^* and Z_2 into Eq. (65), we reproduce the result (41) derived within Wilson's method.

We observe that the analytical effort to derive the coefficients of the ϵ -expansion in this field-theoretical approach is much bigger than that of Wilson's method. Indeed, in the minimal subtraction scheme additional calculations are

needed to extract the coefficients of the ϵ poles of the Feynman diagrams in Figs. 3 and 4. It follows that for an automatized implementation of the high-order ϵ -expansion, Wilson's method turns out to be much better performing than the field-theoretical method. Notwithstanding this, the tensorial operations needed to compute the Q -dependence of the diagrams in this field-theoretical approach turn out to be exactly the same as those needed in Sec. II, and no additional effort has been required to compute them.

IV. CONCLUSIONS

In a previous work [26], we set up two perturbative approaches to compute the IR behavior of a strongly frustrated non-mean-field spin-glass system, the HEA model. The two methods are based on the replica approach, and in particular on the assumption that the physics of the system is encoded in the limit where the number of replicas n tends to zero. Within the ϵ -expansion framework, the two approaches yield the same prediction at two loops for the critical exponent ν related to the divergence of the correlation length.

In this work the two-loop computation is shown in all its most relevant details, so that the reader can reproduce it. Moreover, we show the underlying renormalization group ideas implemented in the two computation methods. One of these is the existence of a characteristic length ξ diverging at

the IR critical fixed point, where the theory is invariant with respect to reparametrization of the length scale.

In addition, we show with an explicit example that such a computation of the critical exponents could be quite easily automatized, i.e., implemented in a computer program, in order to compute high orders of the ϵ -expansion, and so eventually make this theory physically predictive. Indeed, we give a graphical interpretation of the cumbersome tensorial operations needed to compute ν and previously used in Ref. [26]. Such a graphical method makes the calculations much more straightforward and suitable for an implementation in a computer program to compute high orders of the ϵ series. We observe that once this high-order series in ϵ will be known, some resummation technique will be needed to make the theory predictive, because the series probably has a nonconvergent behavior. If the high-order series could be made convergent by means of some appropriate resummation technique, this calculation would yield an analytical control on the critical exponents, resulting in a precise prediction for a non-mean-field spin glass mimicking a real system.

ACKNOWLEDGMENT

We thank N. Sourlas, S. Franz, and M. Mézard for interesting discussions and suggestions.

-
- [1] M. Mézard, G. Parisi, and M. A. Virasoro, *Spin Glass Theory and Beyond* (World Scientific, Singapore, 1987).
 - [2] T. Castellani and A. Cavagna, *J. Stat. Mech.* (2005) P05012.
 - [3] G. Parisi, *J. Phys. A* **13**, 1101 (1980).
 - [4] B. Derrida, *Phys. Rev. Lett.* **45**, 79 (1980).
 - [5] W. L. McMillan, *J. Phys. C* **17**, 3179 (1984).
 - [6] A. J. Bray and M. A. Moore, *Phys. Rev. Lett.* **58**, 57 (1987).
 - [7] D. S. Fisher and D. A. Huse, *Phys. Rev. B* **38**, 373 (1988).
 - [8] T. R. Kirkpatrick, D. Thirumalai, and P. G. Wolynes, *Phys. Rev. A* **40**, 1045 (1989).
 - [9] C. De Dominicis and I. Giardinà, *Random Fields and Spin Glasses: A Field Theory Approach* (Springer, Berlin, 2006).
 - [10] J. H. Chen and T. C. Lubensky, *Phys. Rev. B* **16**, 2106 (1977).
 - [11] G. Kotliar, P. W. Anderson, and D. L. Stein, *Phys. Rev. B* **27**, 602 (1983).
 - [12] J. Zinn-Justin, *Int. Ser. Monogr. Phys.* **113**, 1 (2002).
 - [13] K. G. Wilson and J. B. Kogut, *Phys. Rept.* **12**, 75 (1974).
 - [14] I. Giardinà (private communication).
 - [15] F. J. Dyson, *Commun. Math. Phys.* **12**, 91 (1969).
 - [16] P. Collet and J. Eckmann, *Lect. Notes Phys.* **74** (1978).
 - [17] P. Collet and J. Eckmann, *Commun. Math. Phys.* **55**, 67 (1977).
 - [18] M. Cassandro and G. Jona-Lasinio, *Adv. Phys.* **27**, 6 (1978).
 - [19] A. Theumann, *Phys. Rev. B* **21**, 2984 (1980).
 - [20] A. Theumann, *Phys. Rev. B* **22**, 5441 (1980).
 - [21] A. N. Berker and S. Ostlund, *J. Phys. C* **12**, 4961 (1979).
 - [22] E. Gardner, *J. Phys. (Paris)* **45**, 1755 (1984).
 - [23] S. Franz, T. Jörg, and G. Parisi, *J. Stat. Mech.* (2009) P02002.
 - [24] M. Castellana, A. Decelle, S. Franz, M. Mézard, and G. Parisi, *Phys. Rev. Lett.* **104**, 127206 (2010).
 - [25] Y. V. Fyodorov, A. Ossipov, and A. Rodriguez, *J. Stat. Mech.* (2009) L12001.
 - [26] M. Castellana and G. Parisi, *Phys. Rev. E* **82**, 040105(R) (2010).
 - [27] H. G. Katzgraber and A. P. Young, *Phys. Rev. B* **67**, 134410 (2003).
 - [28] H. G. Katzgraber and A. P. Young, *Phys. Rev. B* **72**, 184416 (2005).
 - [29] H. G. Katzgraber, A. K. Hartmann, and A. P. Young, in *Condensed Matter Physics XXI*, edited by D. P. Landau, S. P. Lewis, and H. B. Schuttler (Springer, Heidelberg, 2008).
 - [30] L. Leuzzi, *J. Phys. A* **32**, 1417 (1999).
 - [31] L. Leuzzi, G. Parisi, F. Ricci-Tersenghi, and J. J. Ruiz-Lorenzo, *Phys. Rev. Lett.* **101**, 107203 (2008).
 - [32] G. Parisi and N. Sourlas, *Eur. Phys. J. B* **14**, 3 (2000).
 - [33] Y. Meurice, *J. Math. Phys.* **36**, 1812 (1995).
 - [34] M. Taibleson, *Fourier Analysis on Local Fields* (Princeton University Press, Princeton, NJ, 1976).
 - [35] A. B. Harris, T. C. Lubensky, and J. H. Chen, *Phys. Rev. Lett.* **36**, 415 (1976).
 - [36] M. C. Chang and J. Sak, *Phys. Rev. B* **29**, 2652 (1984).
 - [37] R. Guida and P. Ribeca, *J. Stat. Mech.* (2006) P02007.